

# cADPR Analogues: Effect of an Adenosine 2'- or 3'-Methoxy Group on Conformation

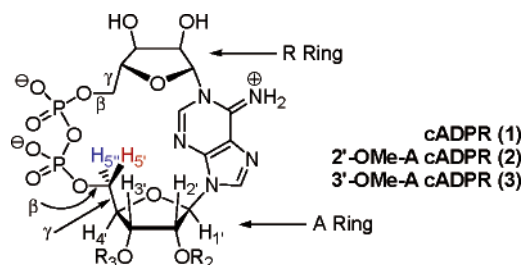
Steven M. Graham,<sup>\*,†</sup> Daniel J. Macaya,<sup>‡</sup> Raghuvir N. Sengupta,<sup>‡</sup> and Kevin B. Turner<sup>†</sup>

Department of Chemistry, St. John's University, Jamaica, New York 11439, and Benjamin N. Cardozo High School, Bayside, New York 11364

grahams@stjohns.edu

Received November 3, 2003

## ABSTRACT



The 2'-OMe-A (2) and 3'-OMe-A (3) analogues of the calcium release agent cADPR (1) were prepared and their solution structures studied by NMR spectroscopy. Compared to 1, 2 shows a shift in its A ring conformation and changes in its R ring N:S and  $\gamma^{\text{A}}:\gamma^{\text{R}}$  ratios, while 3 displays a significant change in the conformation of its A ring  $\gamma$ -bond.

Many small molecules are known to have roles in cell signaling. One such molecule is cyclic adenosine 5'-diphosphate ribose (cADPR, 1), formed in vivo from NAD<sup>+</sup> in a reaction catalyzed by ADP-ribosyl cyclase (ADPRC). Produced in response to extracellular signals, cADPR leads to the release of calcium ions from intracellular stores.<sup>1</sup> cADPR has been found in a variety of organisms and organs, and is involved in diverse cellular processes such as muscle contraction, glucose metabolism, and sea urchin egg fertilization. However, despite the obvious importance of cADPR in cell signaling, the precise mechanism by which cADPR causes calcium release remains poorly understood.

The commercial availability and loose substrate specificity of ADPRC has proved invaluable in the preparation of cADPR analogues. The Potter group prepared cADPR analogues modified in the adenosine furanose ring.<sup>2</sup> They found the analogue without a 2'-OH (2'-dA cADPR) was

essentially as potent as cADPR toward calcium release, whereas 3'-dA cADPR was ~100-fold less potent. A third analogue, where the 3'-OH was replaced with a 3'-methoxy group (3'-OMe-A cADPR, 3), did not cause calcium release but instead blocked the ability of cADPR to release calcium. It was proposed that perhaps the 3'-OH made a hydrogen bond contact critical for recognition.

We had recently determined the NMR solution structure of cADPR<sup>3</sup> and were intrigued by an alternate explanation: that the 2'- and 3'-modifications could be altering the conformation of the furanose ring. To address this issue, we prepared the methoxy analogues 2'-OMe-A cADPR (2) and 3'-OMe-A cADPR (3) to determine the effect, if any, of the methoxy group on cADPR conformation.

The synthesis of cADPR analogues 2 and 3 is shown in Scheme 1. Briefly, 2'-O-Me- or 3'-O-Me adenosine (4 or 5, respectively) were selectively 5'-phosphorylated (POCl<sub>3</sub>/PO-

<sup>†</sup> St. John's University.

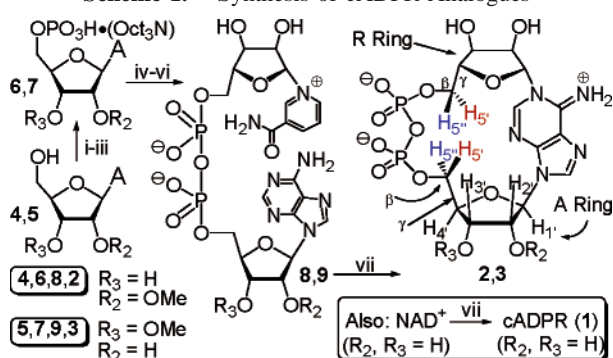
<sup>‡</sup> Benjamin N. Cardozo High School.

(1) (a) Lee, H.-C. *Annu. Rev. Pharmacol. Toxicol.* **2001**, *41*, 317–345.  
(b) Lee, H.-C. *Physiol. Rev.* **1997**, *77*, 1133–1164.

(2) Ashamu, G. A.; Sethi, J. K.; Galione, A.; Potter, B. V. L. *Biochemistry* **1997**, *36*, 9509–9517.

(3) Graham, S. M.; Pope, S. C. *Nucleosides, Nucleotides, Nucleic Acids* **2001**, *20*, 169–183.

### Scheme 1. Synthesis of cADPR Analogues<sup>a</sup>



<sup>a</sup> Reagents and conditions: (i) POCl<sub>3</sub>, TEP; (ii) H<sub>2</sub>O (hydrolysis); (iii) Oct<sub>3</sub>N, MeOH; (iv) DPCP, dioxane, DMF, Bu<sub>3</sub>N; (v) Ac<sub>2</sub>NMN, DMF, pyridine, Bu<sub>3</sub>N; (vi) NH<sub>3</sub>, MeOH; (vii) ADPRC.

(OEt)<sub>3</sub>)<sub>4</sub> isolated as the free acids, and converted to their triethylammonium salts (**6**, **7**). Activation of **6** or **7** toward nucleophilic attack by the 5-phosphate of 2',3'-di-*O*-acetyl nicotinamide mononucleotide (Ac<sub>2</sub>NMN)<sup>5</sup> was performed by using the Michelson procedure (PO(OPH)<sub>2</sub>Cl/Bu<sub>3</sub>N in dioxane/DMF).<sup>5,6</sup> Removal of the acetyl groups (MeOH/NH<sub>3</sub>) followed by ion-exchange chromatography afforded the corresponding NAD<sup>+</sup> analogues **8** or **9** in ~15% overall yield. The NAD<sup>+</sup> analogues and NAD<sup>+</sup> itself were cyclized using ADPRC, purified, and isolated as their sodium salts to give **1–3** in ~65% yield.<sup>7</sup>

We then focused on determining the NMR solution structures of **1–3**. Furanose rings generally exist in a two-state equilibrium; the geometry of each ring is described by a phase angle, *P*, and a puckering amplitude,  $\Phi$ .<sup>8</sup> Rings with *P* = 0 ± 90° are described as “north” (N, or <sup>3</sup>T<sub>2</sub> for *P* = 0); those with *P* = 180 ± 90° are described as “south” (S, or <sup>2</sup>T<sub>3</sub> for *P* = 180)<sup>9</sup> (Figure 1). Also shown in Figure 1 are the defining conformations of the β- and γ-bonds.

The furanose ring, β-bond, and γ-bond conformations and their relative populations were derived from <sup>1</sup>H NMR data. The β- and γ-bond conformations are reflected in the coupling of H<sub>5</sub>/H<sub>5'</sub> to P and to H<sub>4</sub>, respectively. In the β<sup>+</sup> and γ<sup>+</sup> rotamers, P (or H<sub>4</sub>) is gauche to both H<sub>5</sub> and H<sub>5'</sub>, resulting in small, approximately equal coupling of P (or H<sub>4</sub>) to H<sub>5</sub> and to H<sub>5'</sub>. Simple “sum rules” are available for calculating the fractional population of the β<sup>+</sup> and γ<sup>+</sup>

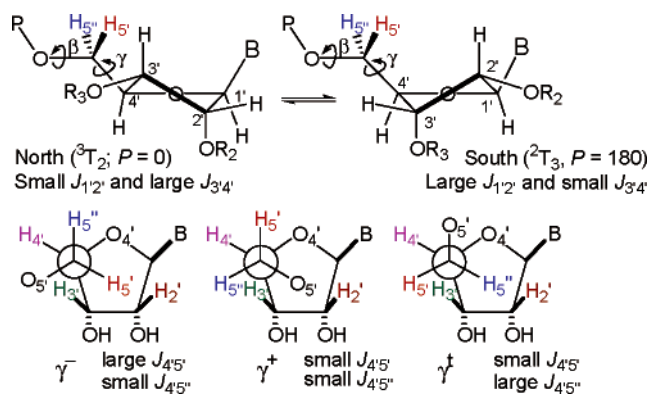


**Figure 1.** The defining atoms for the β- (trans conformation shown) and γ-bonds are C4'-C5'-O5'-P and C3'-C4'-C5'-O5', respectively.

rotamers.<sup>10</sup> The question as to whether the remaining fraction is β<sup>+</sup> or β<sup>-</sup> and γ<sup>+</sup> or γ<sup>-</sup> is more complicated. These rotamers have P (or H<sub>4</sub>) gauche to one H<sub>5</sub> but anti to the other H<sub>5</sub>, leading to one small and one large coupling. Identifying rotamers other than β<sup>+</sup> and γ<sup>+</sup> thus requires the stereospecific assignments of H<sub>5</sub>/H<sub>5'</sub>. The furanose ring conformations were determined with the program PSEUROT,<sup>11</sup> whose basic principles can be understood by examining the furanose H—H torsion angles in Figure 1. In the S conformer, H<sub>1</sub>' and H<sub>2</sub>' are approximately antiperiplanar, resulting in a large *J*<sub>1'2'</sub>, whereas the H<sub>3</sub>'—H<sub>4</sub>' torsion angle is ~90°, yielding a small *J*<sub>3'4'</sub>. The situation is reversed in the N conformer and one observes a small *J*<sub>1'2'</sub> and a large *J*<sub>3'4'</sub>. The PSEUROT program calculates *J* values for various N and S conformers (each characterized by *P* and  $\Phi$ ) and minimizes the difference between these calculated *J* values and the observed *J* values by adjusting *P*<sub>N</sub>, *P*<sub>S</sub>,  $\Phi$ <sub>N</sub>,  $\Phi$ <sub>S</sub>, and the N:S ratio. The sum rules and the principles of pseudorotation, assuming the needed *J* values can be extracted from <sup>1</sup>H NMR data, provide good estimates of the ring, β-, and γ-bond conformations and populations.

<sup>1</sup>H NMR spectra for **1–3** are shown in Figure 2 and the *J* values are summarized in Table 1.<sup>12</sup> Due to overlaps, not all the required *J* values could be extracted directly from the normal 1D <sup>1</sup>H spectrum, and we used 1D TOCSY<sup>13</sup> and phosphorus-decoupled <sup>1</sup>H (<sup>31</sup>P{<sup>1</sup>H}) NMR experiments to extract *J* values from these crowded regions.

The 1D TOCSY sequence allows magnetization transfer from a selectively excited proton to potentially all of the other protons in the spin system, not just adjacent ones. For

(4) Yoshikawa, M.; Kato, T.; Takenishi, T. *Bull. Chem. Soc. Jpn.* **1969**, 42, 3505–3508.

(5) Bailey, V. C.; Sethi, J. K.; Fortt, S. M.; Galione, A.; Potter, B. V. L. *Chem. Biol.* **1997**, 4, 51–61.

(6) Michelson, A. M. *Biochim. Biophys. Acta.* **1964**, 91, 1–13.

(7) Compounds **1–3** gave satisfactory spectral data (UV and <sup>1</sup>H and <sup>31</sup>P NMR). See the Supporting Information.

(8) The phase angle *P* is a description of which atoms are above (endo) and below (exo) the furanose ring plane;  $\Phi$  is a measure of the furanose ring pucker. See: Altona, C.; Sundaralingam, M. *J. Am. Chem. Soc.* **1973**, 95, 2333–2344.

(9) According to the IUPAC/IUB JCBN guidelines, the E/T symbolism is preferable to the C2'-exo-C3'-endo/C2'-endo-C3'-exo descriptions. In the E/T symbolism, E denotes an envelope and T a twist conformation. Subscripts and superscripts denote that the indicated atom has the exo or endo configuration, respectively. See: *Eur. J. Biochem.* **1983** 131, 9–15.

(10) (a) γ-bond:  $f_{\gamma+} = 13.3 - (J_{4'5'} + J_{4'5''})/9.7$ . Altona, C. *Recl. Trav. Chim. Pays-Bas* **1982**, 101, 413–433. (b) β-bond:  $f_{\beta} = 25.5 - (J_{5'P} + J_{5''P})/20.5$ . Lankhorst, P. P.; Haasnoot, C. A. G.; Erkelens, C.; Altona, C. *J. Biomol. Struct. Dyn.* **1984**, 1, 1387–1405.

(11) van Wijk, J.; Haasnoot, C. A. G.; de Leeuw, F. A. A. M.; Huckriede, B. D.; Westra Hoekzema, A. J. A.; Altona, C. *PSEUROT 6.3*; Leiden Institute of Chemistry, Leiden University: Leiden, The Netherlands, 1999.

(12) The accuracy of the  $\delta$  and *J* values was evaluated through spectral simulation. The rms errors in the simulated versus experimental spectra were 0.09, 0.19, and 0.21 Hz for **1**, **2**, and **3**, respectively. See the Supporting Information for simulated spectra and a table of chemical shifts.

(13) Kessler, H.; Oschkinat, H.; Griesinger, C.; Bermel, W. *J. Magn. Reson.* **1986**, 70, 106–133.

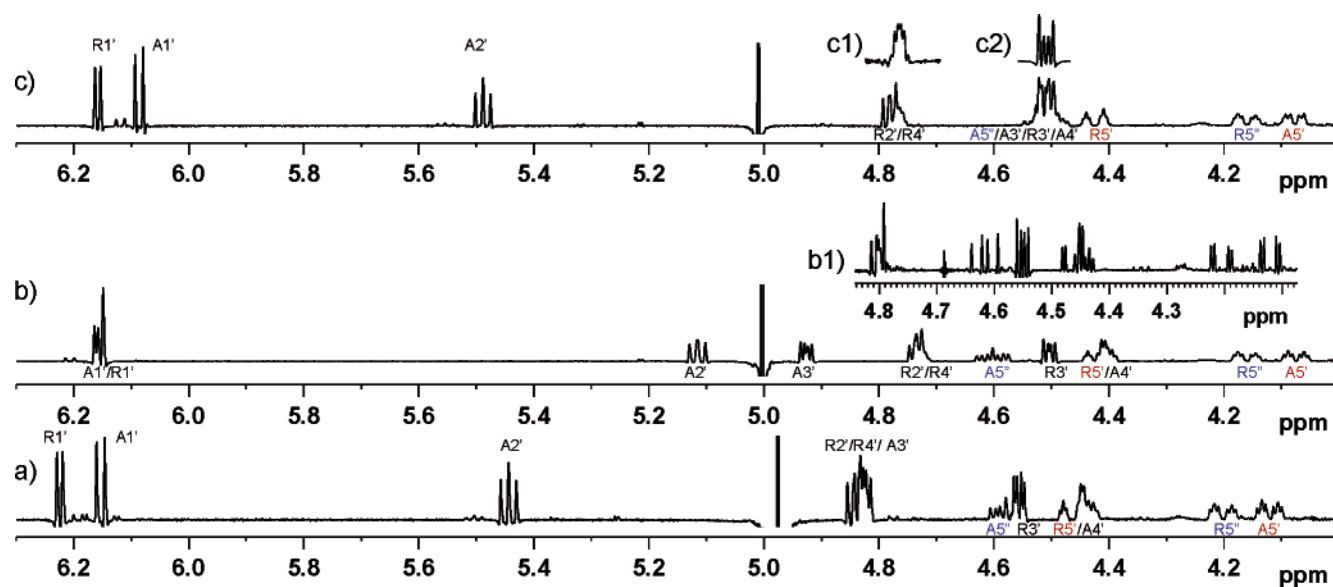


**Figure 2.** 1D  $^1\text{H}$  NMR spectra of (a) **1** (12  $^\circ\text{C}$ ), (b) **2** (6  $^\circ\text{C}$ ), and (c) **3** (6  $^\circ\text{C}$ ) in  $\text{D}_2\text{O}$ . Inset b1:  $\{^{31}\text{P}\}^1\text{H}$  NMR spectrum of **2** (20  $^\circ\text{C}$ ). Insets c1 and c2: 1D TOCSY NMR spectra (6  $^\circ\text{C}$ ) of **3** with excitation at  $\text{R}_5'$  and at  $\text{A}_1'$ , respectively.

example, 1D TOCSY with selective excitation of  $\text{A}_1'$  in **3** (Figure 2) revealed not only the adjacent  $\text{A}_2'$  but also that  $\text{A}_3'$  was a doublet of doublets (dd). Similarly, 1D TOCSY at the upfield  $\text{R}_5$  signal ( $\text{R}_{5u}$ ) clearly showed that  $\text{R}_4'$  was an overlapping doublet of quartets. In the normal 1D  $^1\text{H}$  spectrum,  $\text{R}_4'$  and  $\text{R}_2'$  were overlapped and  $\text{A}_3'$  was obscured by three other signals. The  $\{^{31}\text{P}\}^1\text{H}$  experiment was used to distinguish  $J_{4'5'}/J_{4'5''}$  from  $J_{5'p}/J_{5''p}$  and to identify any four-bond couplings between  $\text{H}_{4'}$  and its 5'-P ( $^4J_{4'p}$ ); couplings lost upon  $^{31}\text{P}$  irradiation were due to  $^{31}\text{P}$ .

The last issue was the stereospecific assignment of  $\text{H}_5'$  and  $\text{H}_5''$ . The standard method<sup>14</sup> is to look for NOEs from  $\text{H}_{3'}$  to  $\text{H}_5'$  and  $\text{H}_5''$ , provided  $\text{H}_{3'}$  is sufficiently isolated to allow selective excitation. Fortunately, 2'-OMe analogue **2** had both  $\text{A}_3'$  and  $\text{R}_3'$  relatively well separated from other signals. Using 1D NOESY,<sup>15</sup> we found that selective irradiation of  $\text{A}_3'$  in **2** led to roughly equal enhancements (1.8% and 2.0%, respectively) of both the downfield  $\text{A}_5$  ( $\text{A}_{5d}$ , therefore  $\text{A}_{5''}$ ) and the  $\text{A}_{5u}$  (therefore  $\text{A}_5'$ ) signals, suggesting an A ring  $\gamma^t$  conformation.<sup>16</sup> The observation of a large  $J_{\text{A}4'5''}$  and a small  $J_{\text{A}4'5'}$  (Table 1) is consistent with this assignment. The R rings in **1–3** all showed  $J_{4'5'} \sim J_{4'5''}$ , consistent only with highly populated R ring  $\gamma^+$  conformers. In this case, irradiation of  $\text{R}_3'$  should enhance only  $\text{R}_5''$ . Interestingly, the downfield/upfield assignments are reversed for the R ring  $\text{H}_5/\text{H}_5''$ , as in **2** it was an NOE from  $\text{R}_3'$  to only  $\text{R}_{5u}$  ( $=\text{R}_5'$ )

that was observed. In cADPR itself, only  $\text{R}_3'$  was sufficiently isolated to selectively irradiate, and it too showed an NOE only to  $\text{R}_{5u}$  ( $\text{R}_5''$ ) and not to  $\text{R}_{5d}$  ( $\text{R}_5'$ ). All additional 1D NOESY experiments carried out on **1** and **3** were consistent with an R ring  $\gamma^+$  and A ring  $\gamma^t$  conformations as the major equilibrium rotamers; the similarity of the  $\text{H}_5/\text{H}_5''$  chemical shifts and  $J$  values also supports the stereospecific assignments.

The PSEUROT furanose geometries,<sup>17</sup> N:S ratios, and the sum rule  $\beta$ -bond and  $\gamma$ -bond rotamer populations are summarized in Table 1. The methoxy group has no effect on the  $\beta$ -bond; the coupling of  $^{31}\text{P}$  to  $\text{H}_5'$  and  $\text{H}_5''$  in all six rings was always small (2.2–4.0 Hz), and all  $\beta$ -bonds are thus almost exclusively  $\beta^t$ . The R ring  $\beta^t$ - $\gamma^+$  conformation leads to a planar “W” arrangement of  $\text{R}_4'$  and its 5'-P and predicts a significant  $^4J_{\text{R}4'p}$ .<sup>10a</sup> **1–3** showed  $^4J_{\text{R}4'p}$  values of 3.5–4.1 Hz. In contrast to the R rings, no  $^4J_{\text{A}4'p}$  couplings were observed in **1–3**, as expected for A ring  $\gamma^t$  conformers.

How does the methoxy group drive the differences in conformation and population? It is well-established<sup>18,19</sup> that highly electronegative (EN) groups at  $\text{C}_2'$  and  $\text{C}_3'$  prefer pseudoaxial orientations, as this places the EN group gauche

(14) Wijmenga, S. S.; Mooren, M. M. W.; Hilbers, C. W. *NMR of Macromolecules: A Practical Approach*; Roberts, G. C. K., Ed.; Oxford University Press: Oxford, UK, 1993; pp 217–288.

(15) Stott, K.; Stonehouse, J.; Keeler, J.; Hwang, T. L.; Shaka, A. J. *J. Am. Chem. Soc.* **1995**, *117*, 4199–4120. This is the “selnpgp.3” pulse program in Bruker’s XWinNMR 2.6.

(16) See the Supporting Information. Further confirmation of the A ring the  $\gamma^t$  conformation was obtained by using 1D NOESY with irradiation at  $\text{A}_2'$  ( $\text{A}_{5d}$  enhanced but not  $\text{A}_{5u}$ ),  $\text{A}_{5d}$  ( $\text{A}_2'$  and  $\text{A}_3'$  enhanced but not  $\text{A}_4'$ ),  $\text{A}_4'$  ( $\text{A}_{5u}$  enhanced but not  $\text{A}_{5d}$ ), and  $\text{A}_{5u}$  ( $\text{A}_3'$  and  $\text{A}_4'$  enhanced but not  $\text{A}_2'$ ).

(17) In the pseudorotational treatment, the two-state conformational equilibrium is described by the following five variables:  $P_N$ ,  $\Phi_N$ ,  $P_S$ ,  $\Phi_S$ , and a mole fraction (of either conformer). Ribofuranoses cannot be completely determined, as there are only three observable values related to the endocyclic torsion angles ( $J_{1'2'}$ ,  $J_{2'3'}$ , and  $J_{3'4'}$ ) and therefore assumptions concerning two of the variables must be made. It has been noted (de Leeuw, F. A. A. M.; Altona, C. *J. Chem. Soc., Perkin Trans. 2* **1982**, 375–384) that there is a correlation of low  $\Phi$  values to high  $J_{2'3'}$  values. In all six rings in **1–3** we observed relatively high  $J_{2'3'}$  values ( $5.05 \pm 0.15$  Hz), and have thus constrained  $\Phi_N$  and  $\Phi_S$  to the relatively low value of  $35^\circ$ . Constraining  $\Phi_N$  and  $\Phi_S$  to  $33^\circ$  and  $37^\circ$  gave similar results. The number of observables can be increased if the  $J$  values change significantly with temperature, but in the limited temperature ranges studied so far cADPR and its analogues show very little variation with temperature. An extensive variable-temperature study and full pseudorotation analysis will be presented in due course.

**Table 1.** Coupling Constants ( $J$ , in Hz) and Structural Parameters for **1–3**<sup>a</sup>

cmpd	A ring $J$										R ring $J$									
	1'2'	2'3'	3'4'	4'P	4'5'	4'5''	5'5''	P5'	P5''	1'2'	2'3'	3'4'	4'P	4'5'	4'5''	5'5''	P5'	P5''		
<b>1</b> <sup>b</sup>	5.8	5.1	3.2	0.0	2.5	6.8	11.0	3.6	3.9	3.9	5.1	2.3	4.1	2.2	2.3	12.0	2.2	3.6		
<b>2</b> <sup>c</sup>	6.0	4.9	2.7	0.0	2.7	7.3	11.0	3.4	3.5	3.5	5.0	3.0	4.2	2.3	2.4	11.8	2.3	3.5		
<b>3</b> <sup>d</sup>	5.6	5.2	3.2	0.0	0.0	6.4	10.4	3.8	4.0	3.8	5.0	2.5	3.5	2.3	2.4	12.1	2.3	3.5		
	$P_N$		$P_S$		N:S		$\gamma^-:\gamma^+$		$\beta^t$		$P_N$		$P_S$		N:S		$\gamma^-:\gamma^+$		$\beta^t$	
<b>1</b> <sup>e</sup>	45° ( <sup>3</sup> T <sub>4</sub> /4E)		191° ( <sub>3</sub> E)		31:69		59:41		> 89%		325° ( <sup>1</sup> T <sub>2</sub> )		207° ( <sub>3</sub> E/ <sup>4</sup> T <sub>3</sub> )		38:62		9:91		> 96%	
<b>2</b> <sup>e</sup>	335° ( <sub>2</sub> E)		162° ( <sup>2</sup> E)		34:66		66:34		> 91%		329° ( <sup>1</sup> T <sub>2</sub> )		204° ( <sub>3</sub> E)		49:51		12:88		> 96%	
<b>3</b> <sup>e,f</sup>	53° ( <sub>4</sub> E)		199° ( <sub>3</sub> E)		32:68		$\gamma^t$		> 87%		327° ( <sup>1</sup> T <sub>2</sub> )		206° ( <sub>3</sub> E)		41:59		11:89		> 96%	

<sup>a</sup> All ring  $J$  values are  $\pm 0.1$  Hz; all backbone  $J$  values are  $\pm 0.2$  Hz. All  $\delta$  and  $J$  values were confirmed by spectral simulation. Values are from 1D <sup>1</sup>H spectrum except where noted. <sup>b</sup> D<sub>2</sub>O, 12 °C.  $J_{A4'P}$  = 0.4 Hz used in simulation.  $J_{A4'A5'}$  from {<sup>31</sup>P}<sup>1</sup>H.  $J_{A5'5''}$  from the 1D spectrum and {<sup>31</sup>P}<sup>1</sup>H. <sup>c</sup> D<sub>2</sub>O, 6 °C. <sup>d</sup> D<sub>2</sub>O, 6 °C. Only  $J_{A1'A2'}$ ,  $J_{R1'R2'}$ ,  $J_{R2'3'}$ ,  $J_{R5'P}$ , and  $J_{R5'R5''}$  are from 1D <sup>1</sup>H spectrum; all others are averaged from 1D <sup>1</sup>H and 1D TOCSY and {<sup>31</sup>P}<sup>1</sup>H. <sup>e</sup>  $\Phi_N$  and  $\Phi_S$  restrained to 35°. <sup>f</sup> The precise  $\gamma^-:\gamma^+$  ratio could not be determined; see text.

to the ring oxygen (“gauche effect”). Methoxy is slightly more EN than –OH,<sup>19a</sup> which predicts, relative to **1**, increases in the percent N for **2** and in the percent S for **3**. While precisely these trends were observed in two free nucleosides,<sup>19a,b</sup> **2** and **3** to some extent apparently resist the substituent effect of the methoxy group. Compared to **1**, the 2'-OMe in **2** had virtually no effect on the A ring N:S ratio but rather drove the A ring S conformer from <sub>3</sub>E to <sup>2</sup>E, the N conformer from approximately <sub>4</sub>E to <sub>2</sub>E, and the  $\gamma^t$  population from 59% to 66%. These A ring changes presumably drive the changes seen in the R ring of **2**, where the N and S conformers and the  $\gamma^t$  population were unchanged but the percent S dropped from 62% to 51%. Clearly there are subtle differences between **1** and **2**, and it will be interesting to see if **2** is active. Comparing **3** to **1**, we found them remarkably similar in all aspects of conformation and population except for the A ring  $\gamma$ -bond conformation. The A<sub>5'</sub> signal, a doublet of triplets pattern in **1** and **2**, has collapsed to a dd pattern. The {<sup>31</sup>P}<sup>1</sup>H NMR experiment unambiguously demonstrated that the lost coupling in **3** was  $J_{A4'A5'}$ , suggesting that the torsion angle between A<sub>4'</sub> and A<sub>5'</sub>, normally  $\sim 60^\circ$ , had approached  $\sim 90^\circ$ , reducing  $J_{A4'A5'}$  to  $\sim 0$  Hz.<sup>20</sup> It seems that the 3'-OMe group, rather than altering the conformation or N:S ratio of the A

ring, instead causes the  $\gamma$ -bond to deviate by  $\sim 30^\circ$  from an ideal  $\gamma^t$  angle of  $\sim 180^\circ$  to a nonideal angle of  $\sim 210^\circ$ . Though still within the  $\gamma^t$  range, a bond angle of  $\sim 210^\circ$  is outside the limited ranges ( $\gamma^t = 180 \pm 8^\circ$ ) over which the  $\gamma$ -bond sum rule<sup>10a,b</sup> is valid. In the case of **3** this sum rule greatly overestimates the amount of  $\gamma^+$ . That the A ring  $\gamma$ -bond has a highly populated  $\gamma^t$  conformation is apparent from the relatively large  $J_{A4'A5''}$  (6.4 Hz) observed, demonstrating that A<sub>4'</sub> and A<sub>5''</sub> remain largely anti. Our working hypothesis is that **3** is a cADPR antagonist not because it has altered A ring or R ring conformations but instead has an altered backbone conformation. The observed changes in conformation and population are difficult to rationalize using the gauche effect. Our results with **2** show that a conformational change in one furanose ring can drive a change in the other ring. Further efforts to elucidate the structure–activity relationships in cADPR, including assessing the activity of **2**, full pseudorotation analysis, modeling, and synthesis of new analogues will be presented in due course.

**Acknowledgment.** This work was funded in part by NIH grant GM 62150 to S.M.G..

**Supporting Information Available:** Experimental details for the synthesis of **1–3**; <sup>1</sup>H, <sup>31</sup>P, {<sup>31</sup>P}<sup>1</sup>H, COSY, selected 1D NOESY, and 1D TOCSY NMR spectra. This material is available free of charge via the Internet at <http://pubs.acs.org>.

OL036152R

(20) More accurately,  $J_{A4'A5'}$  has been reduced to the point where it broadens but does not split the A<sub>5'</sub> signal. In the simulation of **3**, a value of 0.4 Hz for  $J_{A4'A5'}$  seemed to broaden the A<sub>5'</sub> appropriately.

(18) Thibaudeau, C.; Chattopadhyaya, J. *Stereoelectronic Effects in Nucleosides and Nucleotides and their Structural Implications*; Uppsala University Press: Uppsala, Sweden, 1999; pp 19–87.

(19) (a) Thymidine, 64% S; 3'-OMe thymidine, 74% S. Thibaudeau, C.; Garg, N.; Papchikhin, A.; Chattopadhyaya, J. *J. Am. Chem. Soc.* **1994**, *116*, 4038–4043. (b) Adenosine, 36% N; 2'-OMe adenosine, 42% N. Uesugi, S.; Miki, H.; Ikehara, M.; Iwahashi, H. *Tetrahedron Lett.* **1979**, *20*, 4073–4076. (c) Guschlbauer, W.; Jankowski, K. *Nucleic Acids Res.* **1980**, *8*, 1421–1433.